JOURNAL OF VIROLOGY, Nov. 2006, p. 10909–10918 Vol. 80, No. 22
0022-538X/06/$08.00+0 doi:10.1128/JVI.00950-06

Cooperative Involvement of the S1 and S2 Subunits of the Murine Coronavirus Spike Protein in Receptor Binding and Extended Host Range▽

Cornelis A. M. de Haan,* Eddie te Lintelo, Zhen Li,† Matthijs Raaben, Tom Wurdinger, Berend Jan Bosch, and Peter J. M. Rottier

Virology Division, Department of Infectious Diseases and Immunology, Faculty of Veterinary Medicine, and Institute of Biomembranes, Utrecht University, Utrecht, The Netherlands

Received 10 May 2006/Accepted 26 August 2006

To study the process of spike (S)-receptor interaction during coronavirus entry, we evaluated the contributions of mutations in different regions of the murine hepatitis virus (MHV) S protein to natural receptor murine carcinoembryonic antigen-related cell adhesion molecule 1a (CEACAM1a) dependence and to the acquisition of extended host range. Extended-host-range variants of MHV strain A59 were previously obtained from persistently infected cells (J. H. Schickli, B. D. Zelus, D. E. Wentworth, S. G. Sawicki, and K. V. Holmes, J. Virol. 71:9499-9504, 1997). These variant viruses contain several mutations in the S protein that confer to the viruses the ability to enter cells in a heparan sulfate-dependent manner (C. A. de Haan, Z. Li, E. te Lintelo, B. J. Bosch, B. J. Haijema, and P. J. M. Rottier, J. Virol. 79:14451-14456, 2005). While the parental MHV-A59 is fully dependent on murine CEACAM1a for its entry, viruses carrying the variant mutations in the amino-terminal part of their S protein had become dependent on both CEACAM1a and heparan sulfate. Substitutions in a restricted, downstream part of the S protein encompassing heptad repeat region 1 (HR1) and putative fusion peptide (FP) did not alter the CEACAM1a dependence. However, when the mutations in both parts of the S protein were combined, the resulting viruses became independent of CEACAM1a and acquired the extended host range. In addition, these viruses showed a decreased binding to and inhibition by soluble CEACAM1a. The observations suggest that the amino-terminal region of the S protein, including the receptor-binding domain, and a region in the central part of the S protein containing HR1 and FP, i.e., regions far apart in the linear sequence, communicate and may even interact physically in the higher-order structure of the spike.

The entry of enveloped viruses into cells requires attachment of the virion to the host cell, followed by fusion of the viral membrane with a membrane of the target cell. While some viruses contain glycoproteins that mediate both virus-cell attachment and virus-cell fusion, as is the case for coronaviruses, for others, such as paramyxoviruses, these functions are served by different glycoproteins. In both cases, however, the viral fusion proteins undergo dramatic conformational changes upon activation, which are tightly controlled in time and place in order to effect the proper merging of viral and cellular membranes.

Coronaviruses are enveloped viruses that contain a large single-stranded RNA genome of positive polarity. Their envelope accommodates three or four membrane proteins of which the membrane (M), envelope (E), and spike (S) proteins are common to all (reviewed by de Haan and Rottier [15]). The S protein is a relatively large, 1160- to 1452-amino-acid-long type I glycoprotein, trimers of which form the petal-shaped projections on the surface of the virion that give rise to the characteristic corona solis-like appearance. The S proteins from some but not all coronaviruses are cleaved as a late step during their maturation (reviewed by Cavanagh [8]), for which a furin-like enzyme was shown to be responsible in the case of mouse hepatitis virus (MHV) strain A59 (16). The resulting amino-terminal S1 subunit and the membrane-anchored S2 subunit remain noncovalently linked. It has been suggested that the S1 subunit constitutes the globular head, while the S2 subunit forms the stalk-like region of the spike (8, 9).

The two functions of the coronavirus S protein appear to be spatially separated. The S1 subunit (or the equivalent part in viruses with uncleaved S protein) is responsible for receptor binding, and the S2 subunit is responsible for membrane fusion. For MHV, the receptor-binding domain has been mapped to the amino-terminal 330 residues of the S molecule (23, 42). For transmissible gastroenteritis virus (20), human coronavirus 229E (4, 7), and severe acute respiratory syndrome (SARS) coronavirus (1, 44), the receptor-binding domains have also been mapped to the S1 subunit, though to different regions therein. The ectodomain of the S2 subunit contains two heptad repeat (HR) regions (9) (Fig. 1), characteristic of coiled coils, while the fusion peptide (FP) is predicted to be located amino terminally of the first HR region (HR1) (5). Binding of the S1 subunit to the (soluble) receptor has been shown to trigger conformational changes that supposedly fa-

* Corresponding author. Mailing address: Virology Division, Department of Infectious Diseases and Immunology, Yalelaan 1, 3584 CL Utrecht, The Netherlands. Phone: 31-30-2534195. Fax: 31-30-2536723. E-mail: c.a.m.dehaan@vet.uu.nl.

† Present address: Institute of Animal Science and Veterinary Medicine, Shanghai Academy of Agricultural Science, Beidi Road 2901, Shanghai 201106, People's Republic of China.

▽ Published ahead of print on 6 September 2006.

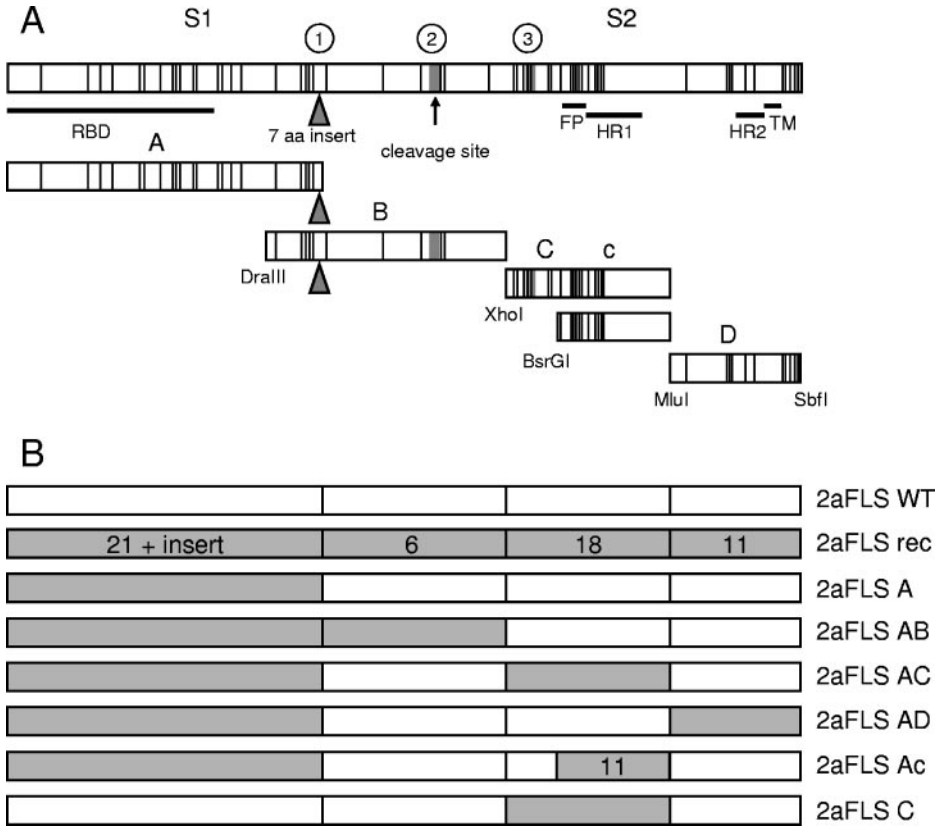

FIG. 1. Cloning strategy and organization of the chimeric S proteins. (A) The spike protein is depicted as an elongated box. Each vertical line in this box indicates an amino acid substitution in the MHV/BHK S protein relative to the parental MHV-A59 spike protein. The triangle indicates a 7-amino-acid (aa) insertion. The position of the arrow marks the position where the MHV-A59 S protein can be cleaved into an amino-terminal S1 and a carboxy-terminal S2 subunit. Horizontal lines designate the approximate locations of the receptor-binding domain (RBD), the putative fusion peptide (FP), heptad repeat regions 1 (HR1) and 2 (HR2), and the transmembrane domain (TM). The circled numbers indicate the locations of the heparan sulfate-binding consensus sequences, which are marked by gray boxes and triangles. Fragments A, B, C, c, and D of the MHV/BHK S protein are indicated. Restriction enzymes used to clone the PCR fragments encoding these fragments are shown. (B) The chimeric S proteins are also depicted as elongated boxes, while the recombinant viruses containing these proteins are specified on the right side. White and gray boxes indicate the parts encoded by MHV-A59 and MHV/BHK, respectively. The numbers in the boxes indicate the number of amino acid differences in this part of the MHV/BHK S protein compared to the MHV-A59 S protein.

cilitate virus entry by activation of the fusion function of the S2 subunit (19, 25, 28, 49). The conformational changes are thought to expose the fusion peptide and to lead to the formation of a heterotrimeric six-helix bundle by the two HR regions, a characteristic of class I viral fusion proteins, resulting in the close locations of the fusion peptide and the transmembrane domain in the process of membrane fusion (5, 6, 17, 37, 45, 46).

The interaction between the coronavirus S protein and its receptor is the main determinant for virus entry and host range restriction. MHV is critically dependent on the murine carcinoembryonic antigen-related cell adhesion molecule 1a (mCEACAM1a) for cell entry and hence infects only murine cells. It was therefore quite remarkable when MHV variants capable of infecting nonmurine cells appeared to develop in persistently infected cell cultures (2, 3, 32, 34). MHV/BHK was isolated from persistently infected 17Cl1 cells (32) that had been passaged for up to 600 times (34). This virus no longer depends on murine CEACAM1a for entry (34) but gained the ability to enter cells in a heparan sulfate-dependent manner (11). The adaptation of the virus to heparan sulfate as an attachment/entry receptor was demonstrated by increased heparin binding as well as by inhibition of infection through treatment of cells and virus with heparinase and heparin, respectively. MHV/BHK differs in its S protein at 57 residues and additionally contains a 7-amino-acid insert compared to its parental A59 strain. Previously, the extended host range was mapped to a domain in the S1 subunit, which contained 21 of the amino acid substitutions and the 7-amino-acid insert (33). These mutations, when placed into an isogenic background permitted MHV-A59 to infect murine and nonmurine cells. However, these viruses failed to induce a second round of infection in nonmurine cells when grown in liquid medium, indicating that additional mutations in the S gene are needed for the extended-host-range phenotype (39).

These studies raise the question how these viruses have acquired their extended-host-range phenotype and how the S protein is triggered to undergo the conformational changes required to initiate the fusion process. In the present study we have demonstrated that a combination of mutations in the S1 and S2 subunits are obligatory for the virus to shift from its specific mCEACAM1a dependence to a relatively unspecific

heparan sulfate-dependent, extended host range. Therefore, although far apart in the linear sequence, the two mutation-containing regions are likely to communicate or to be in close contact in higher-order structures.

MATERIALS AND METHODS

Cells, viruses, and antibodies. *Felis catus* whole-fetus (FCWF) cells (American Type Culture Collection) were used for infection with the interspecies chimeric coronavirus feline MHV (24). Murine LR7 cells (24) were used to propagate the recombinant MHVs. HeLa cells (American Type Culture Collection) were used to test the extended-host-range phenotypes. The generation of the recombinant virus MHV-2aFLS (designated the wild type [WT] here) has been described previously (10). The anti-MHV serum k134 (30) and the monoclonal (CC1; 18) and polyclonal (41) antibodies against mCEACAM1a have also been described before. The latter two were kindly provided by Kay Holmes and Tom Gallagher, respectively. MHV-rec1, which contains the MHV/BHK S gene, was kindly provided by Stan Sawicki.

Plasmid constructs. MHV transcription vectors for the production of donor RNA for targeted recombination were derived from transcription vector pMH54 S21BHK+i (39), which is a derivative of pMH54 (24). pMH54 S21BHK+i specifies a defective MHV-A59 RNA transcript consisting of the 5′ end of the genome (467 nucleotides) fused to codon 28 of the hemagglutinin esterase (HE) gene and running to the 3′ end of the genome, in which approximately 1,500 nucleotides at the 5′ end of the MHV-A59 S gene (GenBank accession number AY497328) have been exchanged by the corresponding sequence of the MHV/BHK S gene (GenBank accession number AY497331). A firefly luciferase expression cassette was cloned into pMH54 S21BHK+i at the position of the HE pseudogene exactly as described previously (10), resulting in pFLS21+i, which was subsequently used for the construction of MHV-2aFLS A. Subsequently, other parts of the MHV-A59 S gene in pFLS21+i were exchanged with the corresponding parts of the MHV/BHK S gene. To this end, parts of the MHV/BHK S gene (containing fragments B, C, c, and D in Fig. 1) were amplified by reverse transcriptase PCR by using primer combinations 2462 (5′-GTCTCGAG CTTATAGTAACAC-3′; corresponding to the sequence in the S gene with a unique XhoI site) and 2259 (5′-CAGCTTGGTAACTCTGGATT-3′; complementary to a sequence just upstream of an unique DraIII site in the S gene), 2461 (5′-GTGTTACTATAAGCTCGAGAC-3′; corresponding to the sequence in the S gene with the unique XhoI site) and 2460 (5′-CCTGCAGGTGATAGTCAA TCTTCATGAGAGG-3′; complementary to a sequence at the extreme 3′end of the S gene and introducing an SbfI site), and 2040 (5′-GCGGATCCCAATAT AGAATTAATGGTTTAG-3′; corresponding to a sequence upstream of a unique MluI site in the S gene) and 2460. The PCR-amplified fragments were cloned into pGEM-T Easy (Promega) and verified by sequencing. The sequences were identical to the published sequence (GenBank accession number AY497331) except for the presence of two silent mutations in the B fragment. Fragments B, C, c, and D were cloned into plasmid pFLS21+i or pXH2aFLS (10) either alone or in combination using the restriction enzymes indicated in Fig. 1, resulting in the transcription vectors used to construct the recombinant viruses MHV-2aFLS rec, AB, AC, Ac, AD, and C.

Generation of recombinant viruses. Incorporation of the expression cassettes and the S-gene mutations into the MHV genome by targeted recombination was carried out as described previously (12). Briefly, donor RNAs transcribed from linearized MHV transcription vectors were electroporated into *Felis catus* whole-fetus cells that had been infected earlier with feline MHV. The electroporated cells were then plated on a monolayer of LR7 cells for the propagation of the recombinant MHVs. After 24 to 48 h of incubation at 37°C, progeny viruses released into the culture medium were harvested and purified twice using end-point dilutions on LR7 cells before a passage 1 stock was grown. After confirmation of the recombinant genotypes by reverse transcriptase PCR on purified genomic RNA, a passage 2 stock was grown, which was subsequently used in the experiments. In all cases, two independent recombinant viruses were generated to verify that the observed phenotypic characteristics were the result of the intended genomic modifications.

Determination of firefly luciferase (FL) expression. LR7 or HeLa cell monolayers grown in 96-well plates were infected with 5×10^4 50% tissue culture infective dose ($TCID_{50}$) units of the recombinant MHVs as determined on LR7 cells (multiplicity of infection [MOI] of 1). At the indicated times, the culture medium was removed, and cells were lysed using the appropriate buffer provided with the firefly luciferase assay system (Promega). Intracellular luciferase expression was measured according to the manufacturer's instructions, and relative light units were determined in a Turner Designs TD-20/20 luminometer.

Immunocytochemistry. LR7 or HeLa cell monolayers were fixed, permeabilized, and processed for immunocytochemistry as described previously (11). Peroxidase was visualized using an 3-amino-9-ethyl-carbazole substrate kit from Vector Laboratories. Pictures were taken using bright-field microscopy and a Nikon DS-L1 digital camera.

Inhibition experiments. LR7 or HeLa cell monolayers in 96-well plates were incubated at 37°C with the monoclonal (CC1) or polyclonal antibodies against mCEACAM1a at 1:10 or 1:50 dilution, respectively. After 1 h, the recombinant viruses were added to the wells (MOI of 1). Treatment of the cells with heparinase I (Sigma) or incubation of the viruses with heparin (ICN Biochemicals) was performed as described previously (11). Briefly, cells were pretreated with different concentrations of heparinase I at 37°C prior to inoculation of the cells. After 1.5 h, the recombinant viruses (5×10^4 $TCID_{50}$ units) were added to the wells. Recombinant viruses (10^6 $TCID_{50}$ units/ml Dulbecco's modified Eagles medium [DMEM]) were incubated with different concentrations of heparin for 1 h at 4°C. After the incubation, cell monolayers in 96-well plates were inoculated with the virus-heparin mixtures (5×10^4 $TCID_{50}$ units per well). The infection inhibition experiments with soluble mCEACAM1a (sMHVR-Ig; expression construct kindly provided by Tom Gallagher [19]) were performed essentially as described for the heparin inhibition experiments, except that the viruses were incubated with different concentrations of purified soluble receptor instead of heparin. At 5 h (LR7 cells) or 7 h (HeLa cells) postinfection, the cells were washed with phosphate-buffered saline (PBS) and lysed, and the luciferase expression levels were determined. All experiments were performed at least twice and in triplicate. The results from representative experiments are shown.

Soluble mCEACAM1a binding experiments. Radiolabeled virions were prepared by metabolic labeling of LR7 cells with ^{35}S in vitro labeling mix (Amersham) after being infected with the recombinant viruses as described before (12). Affinity isolations of the radiolabeled virions with the anti-MHV serum k134 were carried out by performing immunoprecipitations in the absence of detergents followed by sodium dodecyl sulfate-15% polyacrylamide gel electrophoresis as described before (14). The amount of M protein precipitated was quantitated using a phosphorimager and used as a measure for the amount of radiolabeled virions. Subsequently, affinity isolations were performed at 4°C with similar amounts of radiolabeled virions and with different concentrations of soluble mCEACAM1a or with the anti-MHV serum. The purified virions were analyzed by electrophoresis, and the amount of M protein precipitated was quantitated using a phosphorimager and normalized to the amount of M protein precipitated with the anti-MHV serum (the amounts were very similar for the different recombinant viruses).

Temperature stability experiments. Recombinant viruses (10^6 $TCID_{50}$ units/ml DMEM) were incubated at 4 or 37°C prior to inoculation of the LR7 cells (96-well plate; 5×10^4 $TCID_{50}$ units per well). Before the incubation, the pH of the DMEM had been adjusted to approximately 6.5 and 8.2 by the addition of morpholineethanesulfonic acid (MES) (pH 5; 20 mM final concentration) or Tris-HCl (pH 8.5; 20 mM final concentration), respectively. At 5 h postinfection, the cells were washed with PBS and lysed, and the luciferase expression levels were determined.

RESULTS

Generation of recombinant viruses. In our previous study (11), we established that heparan sulfate functions as an entry receptor of the extended-host-range variant of MHV generated by Sawicki and Schickli and coworkers (MHV/BHK) (32, 34). In addition, we demonstrated that the S gene of MHV/BHK is sufficient to confer the extended-host-range phenotype (11). This was accomplished by the generation of viruses differing only in their S-gene sequences. Thus, while MHV-2aFLS WT (10) contains the parental MHV-A59 S gene, MHV-2aFLS rec has the MHV/BHK S gene (11) (Fig. 1) in the isogenic MHV-A59 background. Only the latter recombinant virus was able to infect nonmurine cells. Here we extended these observations by the generation of an elaborate set of recombinant viruses that again differ only in their S-gene sequences. In fact, the viruses contain different chimeras of the MHV-A59 and the MHV/BHK S genes. In addition, a firefly luciferase expression cassette (13) was inserted at the position

TABLE 1. Infectivity of viruses in murine and human cells

MHV-2aFLS virus	Infectivity ($TCID_{50}$/ml)[a]		Ratio[b]
	LR7 cells	HeLa cells	
WT	5.1×10^7	≤63	≥8.1×10^5
rec	3.2×10^7	2.5×10^6	13
A	4.6×10^8	≤63	≥7.3×10^6
AB	5.3×10^8	≤132	≥4.0×10^6
AC	8.5×10^7	6.2×10^6	14
AD	1.9×10^9	≤63	≥3.0×10^7
Ac	2.1×10^8	2.2×10^5	960
C	6.8×10^6	≤63	≥1.1×10^5

[a] The viral infectivity in passage 2 stocks was determined by a quantal assay on LR7 (murine) and HeLa (human) cells, and their $TCID_{50}$ values were calculated. The mean value of two independent recombinants is shown.
[b] The ratio of the $TCID_{50}$ values on LR7 and HeLa cells is calculated.

of the HE pseudogene to facilitate analysis (10). Recombinant viruses in which the amino-terminal half of the S1 subunit was from MHV/BHK were found earlier unable to efficiently enter nonmurine cells (39). The present study started with the generation of a similar recombinant virus (MHV-2aFLS A; Fig. 1B). Subsequently, other regions of the MHV/BHK S gene were introduced into the MHV-A59 background in addition to the exchange of the 5′ region (designated region A [Fig. 1A]), resulting in the recombinant viruses MHV-2aFLS AB, AC, AD, and Ac). Finally, a recombinant virus was generated that does not contain the mutations in the amino-terminal part of the S protein but carries only the mutations found around the HR1 region of the MHV/BHK S protein (MHV-2aFLS C).

Infection of murine cells. The infection characteristics of the recombinant viruses were first analyzed on murine LR7 cells. As a first step, the viral infectivity in the passage 2 stocks was determined by a quantal assay, and their $TCID_{50}$ values were calculated (Table 1). All passage 2 stocks, which were used in the subsequent experiments, showed similar titers on the LR7 cells (Table 1), indicating that all recombinant viruses replicated efficiently in these cells. Next, the growth characteristics of the recombinant viruses were compared in more detail. Cultures of LR7 cells infected with the different viruses at an MOI of 1 were lysed at 6.5 and 8.5 h postinfection after which the luciferase expression levels were determined (Fig. 2A). From our previous work, we know luciferase expression to peak at 8 to 9 h postinfection (13). Although some differences were observed, the recombinant viruses appeared to express rather similar levels of luciferase at both time points, indicating that their ability to enter LR7 cells was not affected strongly by the changes in the spike protein.

On the other hand, however, the recombinant viruses appeared to exhibit clear differences in their ability to form plaques (Fig. 2B). While infection with MHV-2aFLS WT resulted in the formation of large syncytia, no cell-cell fusion was observed with MHV-2aFLS rec, and only single cells were infected. It appeared that all viruses with chimeric spikes displayed plaques smaller than those of MHV-2aFLS WT. Cleavage of the MHV-A59 S protein is known to dramatically enhance cell-cell fusion (16). While the S protein of MHV-2aFLS WT is cleaved, that of MHV-2aFLS rec is not (11). The lack of cleavage appeared to correlate with the exchange of the B fragment as was demonstrated by metabolic labeling of infected cells followed by immunoprecipitation using MHV-specific antibodies (data not shown). The absence of cleavage probably explains the poor cell-cell fusion observed for MHV-2aFLS AB compared to MHV-2aFLS A. Some recombinant viruses that did not contain the B fragment and hence contained S proteins that were cleaved to the same extent as MHV-2aFLS WT also demonstrated a reduced cell-cell fusion phenotype (for instance, MHV-2aFLS C). Apparently, mutations in fragment C, which comprises regions (HR1 and the putative FP) known to be important in the fusion process, can also affect cell-cell fusion. These observations present yet another example showing that virus-cell and cell-cell fusion are processes with different requirements (16, 47).

Infection of human cells. Next we analyzed the extended-host-range phenotypes of the recombinant viruses. Therefore, the viral infectivities in the passage 2 stocks were now determined on HeLa cells (Table 1). Although the recombinant viruses displayed similar titers on the LR7 cells, a clear difference was observed after inoculation of the HeLa cells. Titers could be obtained only for MHV-2aFLS rec, AC, and Ac. The common feature of these three recombinants is the presence of mutations in the amino-terminal part of the S1 subunit (region A) and in a restricted region of the S2 subunit containing the HR1 and the putative FP (region c). Additional mutations in the region immediately upstream thereof (present in region C)

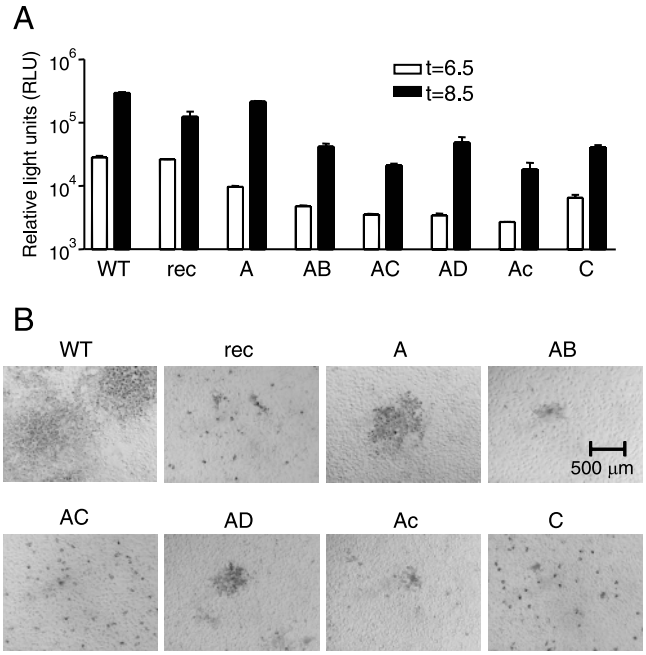

FIG. 2. Infection of murine cells. (A) LR7 cells were inoculated with the indicated recombinant viruses (MHV-2aFLS WT, rec, A, etc.) at an MOI of 1. At the indicated time points postinfection, the cells were lysed and the intracellular luciferase expression was determined by using a luminometer (values are expressed in relative light units [RLU]). Standard deviations (error bars) are indicated. (B) Plaque phenotypes of the recombinant viruses on LR7 cells. At 18 h postinfection, cells were fixed with a 3% formaldehyde solution after which the agar overlay was removed. After permeabilization with 1% Triton X-100 in PBS, viral antigen was detected with the anti-MHV serum k134. Peroxidase-conjugated swine immunoglobulins to rabbit immunoglobulins (Dakopatts) were used as secondary antibodies.

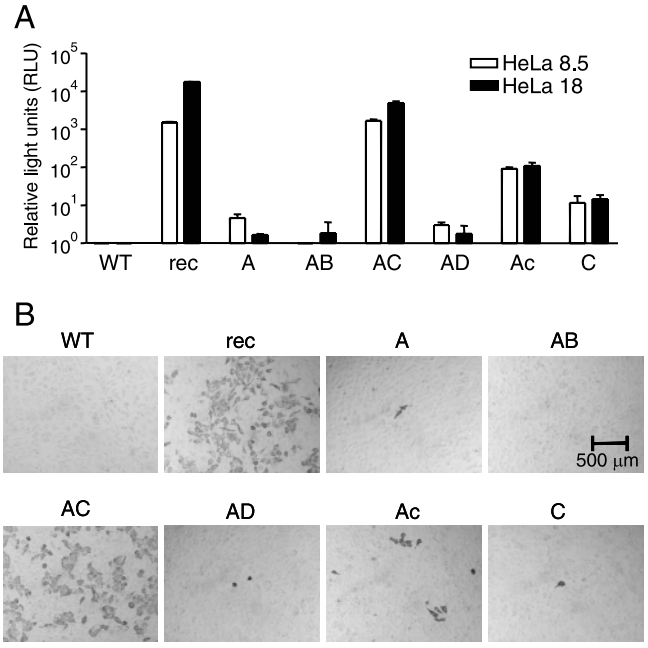

FIG. 3. Infection of human cells. (A) HeLa cells were inoculated with the indicated recombinant viruses (MHV-2aFLS WT, rec, A, etc.), and the intracellular luciferase expression was determined as described in the legend to Fig. 2A. Values for recombinant viruses entering HeLa cells 8.5 and 18 hours postinfection are shown. (B) HeLa cells were infected with the recombinant viruses as described in the legend to Fig. 2B. At 18 h postinfection, the cells were fixed, and viral antigen was detected as described in the legend to Fig. 2B.

increased the relative infectivity on HeLa cells more than 50-fold, as judged from the ratio of the infectious titers on the murine and human cells. The results show that the two recombinant viruses that contain two putative heparan sulfate-binding sites not present in MHV-A59 (sites 1 and 3 in Fig. 1A) (11) were most effective in facilitating HeLa cell entry. The absence of the heparan sulfate-binding site immediately upstream of the FP reduced viral infectivity on HeLa cells, although this site was not essential for obtaining an infectious titer, indicating that mutations in the region containing the FP and HR1 also play an important role in the acquisition of the extended host range.

Subsequently, the infection characteristics of the recombinant viruses on HeLa cells were analyzed in more detail. Cultures of HeLa cells infected at an MOI of 1, as defined by $TCID_{50}$ assay on LR7 cells, with the different recombinants were lysed at 8.5 and 18 h postinfection after which the luciferase expression levels were determined. While the differences in the spike protein hardly affected the ability of MHV to enter LR7 cells (Table 1 and Fig. 2A), large variations in luciferase expression levels were observed after inoculation of HeLa cells (Fig. 3A). As expected from their infectious titers obtained on HeLa cells, MHV-2aFLS rec and MHV-2aFLS AC showed the highest luciferase expression levels, while those of MHV-2aFLS Ac were considerably lower. The other recombinant viruses were able to infect the HeLa cells only to a very low extent, with the exception of MHV-2aFLS WT, which could not infect these cells at all. Luciferase levels of MHV-2aFLS rec and AC increased from 8.5 to 18 h postinfection, reflecting the spread of the virus through the cell cultures. These results were confirmed by immunocytochemistry using the MHV antiserum on HeLa cells at 18 h postinfection (Fig. 3B). These data confirm and extent the results shown in Table 1. Viruses containing the mutations in either region A or C infect HeLa cells very poorly. Only when there are mutations in both regions does entry into HeLa cells become much more efficient.

Spike-CEACAM1a interaction. Binding to the (soluble) CEACAM1a receptor has been shown to trigger conformational changes in the MHV S1 domain that probably enable virus entry by activation of the fusion function of the S2 domain (19, 25, 28, 49). Similar conformational changes are also expected to be required for mCEACAM1a-independent but heparan sulfate-dependent infection of MHV. Indeed, infection by all recombinant viruses could be efficiently inhibited by a peptide (6) corresponding to the MHV-A59 HR2 region (data not shown), indicating that the fusion mechanism is basically the same irrespective of the receptor used. The set of recombinant viruses described here gave us the opportunity to study which regions of the S protein are responsible for the observed receptor dependencies and to what extent the different recombinant viruses are dependent on or triggered by either mCEACAM1a or heparan sulfate.

Previously it has been demonstrated that infection with MHV-A59, but not MHV/BHK, could be blocked by antibodies binding to mCEACAM1a (34, 39). We performed similar experiments with our set of recombinant viruses. LR7 and HeLa cells were incubated with either a polyclonal (41) or monoclonal (CC1) (18) antibody against mCEACAM1a. After 1 h, viruses were added to the culture supernatant. The cultures were lysed at 5 or 7 h postinfection for the LR7 or HeLa cells, respectively. Luciferase expression was used as a measure of infection. The results (Fig. 4) show that infection by all viruses except MHV-2aFLS rec, AC, and Ac was (almost) completely blocked by the antibodies, indicating that only these latter viruses can enter LR7 cells in a mCEACAM1a-independent manner. Nonspecific effects of the antibody incubations were excluded by using control antibodies and by showing the undisturbed entry of MHV-2aFLS rec in HeLa cells in the presence of the anti-mCEACAM1a antibodies. The significant inhibition of MHV-2aFLS rec infection on LR7 cells, but not on HeLa cells, however, indicates that this virus enters LR7 cells in a manner that is to some extent dependent on CEACAM1a. Viruses that contained the mutations found in region A of the MHV/BHK spike protein but lacked the mutations in region C were unable to enter LR7 cells in a mCEACAM1a-independent manner. Mutations in both regions are required and sufficient for mCEACAM1a-independent entry into cells.

We also studied the interaction between mCEACAM1a and the different recombinant viruses by analyzing the inhibition of virus infection by soluble mCEACAM1a. Previously, it was demonstrated that infection by MHV-A59 but not MHV/BHK could be inhibited by soluble mCEACAM1a (34). A similar experiment was performed in this study. The recombinant viruses were incubated with different concentrations of soluble receptor at 4°C, after which LR7 cells were infected with the receptor-virus mixtures at an MOI of 1. The results are shown in Fig. 5A. The different recombinant viruses clearly differed in their sensitivity to soluble mCEACAM1a. MHV-2aFLS WT

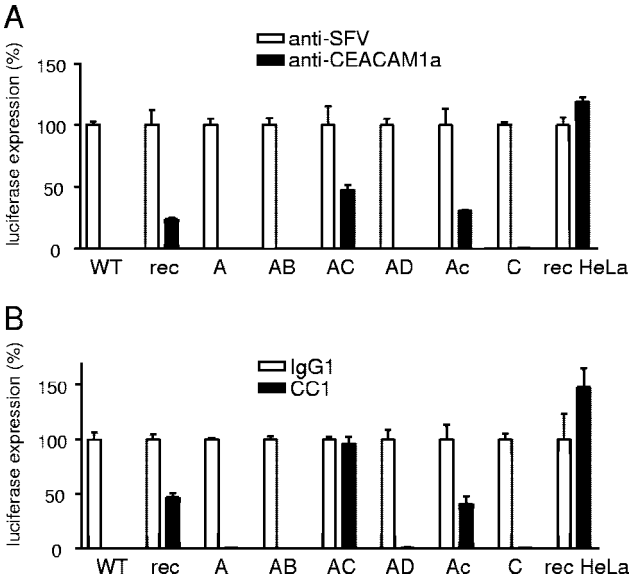

FIG. 4. Inhibition of MHV infection by anti-mCEACAM1a antibodies. (A) LR7 and HeLa cells were inoculated with the recombinant viruses (MHV-2aFLS WT, rec, A, etc.) as described in the legend to Fig. 2A, except the cells had been pretreated with the polyclonal (41) (A) or CC1 monoclonal (18) (B) antibody against mCEACAM1a (or control antibody) for 1 h prior to the inoculation. The control antibodies used were a polyclonal rabbit antiserum against Semliki Forest virus (anti-SFV) and a mouse immunoglobulin G1 (IgG1) isotype control antibody. The relative luciferase expression levels in the cultures are shown. For each individual recombinant virus, the luciferase expression level after pretreatment with the control antibodies was set at 100%. Standard deviations (error bars) are indicated.

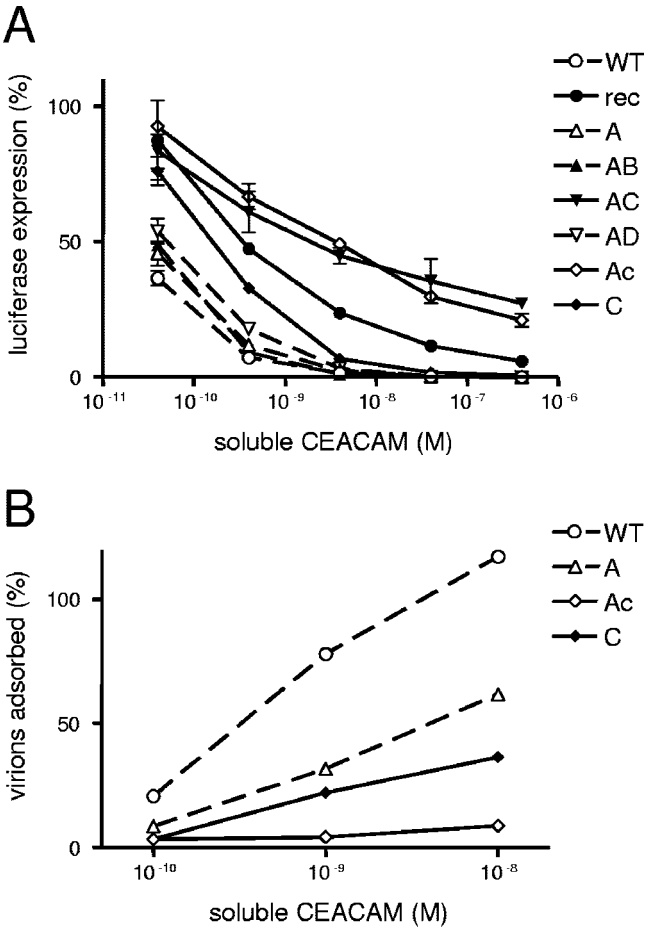

FIG. 5. Interaction of recombinant viruses with soluble mCEACAM1a. (A) Recombinant viruses (MHV-2aFLS WT, rec, A, etc.) were incubated with different concentrations of soluble mCEACAM1a (19), after which the virus-soluble receptor mixtures were used to inoculate LR7 cells. The relative luciferase expression levels in the cultures measured at 5 h postinfection are shown. For each individual recombinant virus, the luciferase expression level observed after mock incubation with soluble mCEACAM was set at 100%. Standard deviations (error bars) are indicated. (B) Radiolabeled virions were incubated with different concentrations of soluble mCEACAM1a after which the amounts of bound virus were determined. The relative amounts of affinity-purified virions are shown. The amount of radioactivity affinity purified from each virion preparation using the MHV antiserum K134 was defined as 100%.

was the most sensitive. Inhibition of virus entry appeared to be influenced more by the mutations in the FP/HR1 (C) region than by the mutations in the amino-terminal (A) region. However, inhibition was least when the mutations in both regions were combined (MHV-2aFLS rec, AC, and Ac). MHV-2aFLS rec appeared to be more sensitive than MHV-2aFLS AC and Ac, indicating perhaps that mutations in region B also affect interaction with the soluble receptor when present in combination with the mutations in the other regions.

Next we evaluated whether this inhibition of virus infection by soluble mCEACAM1a correlated with binding of virus particles to mCEACAM1a. Therefore, similar amounts of radiolabeled virions were incubated with the soluble receptor at 4°C. The soluble receptor contains a Fc tail (19), making it possible to purify virions adsorbed to the soluble receptor by using immobilized protein A. The recombinant viruses that we selected for this assay contained spike proteins lacking mutations in the B region, as these are cleaved to similar extents and cover the whole spectrum of soluble mCEACAM1a-inhibited infection. The affinity-purified viruses were comparatively quantitated by measuring the relative amounts of their M proteins as described in Materials and Methods. The results clearly show that MHV-2aFLS WT bound most efficiently to the soluble receptor (Fig. 5B). Binding was affected significantly by the mutations in both the amino-terminal part of the S1 subunit (MHV-2aFLS A) and those in the central part of the S2 subunit (MHV-2aFLS C). However, binding to soluble mCEACAM1a was most affected when virions contained S proteins with mutations in both regions (MHV-2aFLS Ac). Despite the very different nature of the soluble mCEACAM1a infection-inhibition and the receptor-binding experiments, which were performed at different temperatures (37 and 4°C) and with different amounts of virions, the results of the binding experiments correlate well with those of the infection-inhibition experiments and indicate that the decreased inhibition of infection by soluble mCEACAM1a can be largely attributed to a reduced binding of virions to the receptor. The results further indicate that an interplay of two separate regions in the S protein is responsible for the observed phenotypes.

Temperature stability. Binding of MHV S to its receptor induces conformational changes, which can be mimicked by incubation at 37°C under alkaline conditions (43, 49). These

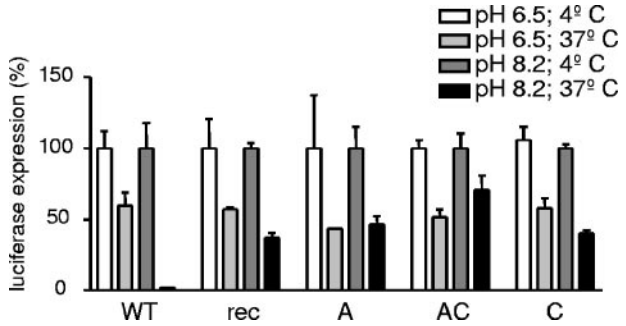

FIG. 6. Temperature- and pH-dependent stability. Recombinant viruses (MHV-2aFLS WT, rec, A, etc.) were incubated at 4 or 37°C at pH 6.5 or 8.2 prior to inoculation of LR7 cells. The relative luciferase expression levels in the cultures measured at 5 h postinfection are shown. For each individual recombinant virus, the luciferase expression level observed after incubation at 4°C for each pH was set at 100%.

conformational changes result in a markedly reduced infectivity of the virus (36). The effects of this temperature and pH-triggered conformational change can easily be monitored by the use of our luciferase-expressing viruses. Thus, the recombinant viruses were incubated either at pH 6.5 or at pH 8.2 both at 4°C and at 37°C for 1.5 h, after which LR7 cells were infected at an MOI of 1. The cultures were lysed at 5 h postinfection to determine the luciferase expression levels. The results (Fig. 6) show that while MHV-2aFLS WT was highly sensitive to incubation at 37°C at pH 8.2, recombinant MHVs that contained either the mutations in the A or C region were much less affected. These viruses exhibited quite a similar temperature stability at pH 8.2 and 6.5. Mutations found in regions B and D did not appear to have an additional effect on the temperature stability (data not shown).

Heparan sulfate dependence. It was also of interest to determine the S-protein requirements of the heparan sulfate-dependent cell entry. Previously we identified two putative heparan sulfate-binding sites in the MHV/BHK S protein not present in the parental sequence (sites 1 and 3 in Fig. 1A). Furthermore, the furin consensus sequence, which is present in both MHV-A59 and MHV/BHK, also contains a heparan sulfate-binding consensus sequence (11, 26). In order to test the involvement of heparan sulfate in the entry process of the different recombinant viruses, LR7 cells were treated with a heparan sulfate-degrading enzyme (heparinase I) for 1.5 h prior to inoculation. This treatment appeared to reduce the entry of all recombinant viruses containing the mutations in the amino-terminal part of the S1 subunit by 50 to 70% (Fig. 7A). The incomplete inhibition might be explained by the presence of heparinase-resistant oligosaccharides (26). Strikingly, luciferase expression by MHV-2aFLS WT and MHV-2aFLS C was increased approximately 2.5-fold after heparinase I treatment. These results were extended by experiments in which the ability of heparin, a competitive inhibitor of heparan sulfate interactions, to reduce viral infectivity was tested. Incubation of the recombinant viruses with heparin prior to inoculation dramatically decreased the infectivities of most recombinant MHVs. The infectivity of MHV-2aFLS WT and MHV-2aFLS C (Fig. 6B) was hardly affected, while MHV-2aFLS AB displayed an intermediate phenotype. The results

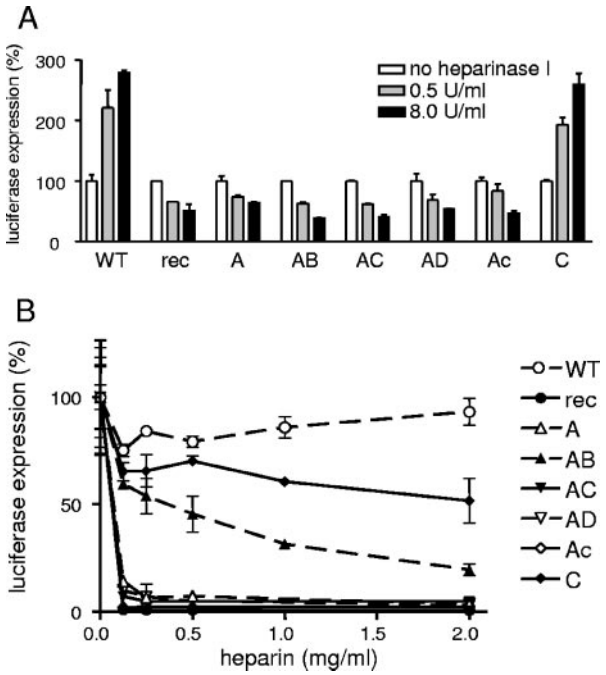

FIG. 7. Heparan sulfate-dependent entry. LR7 cells were inoculated with the recombinant viruses (MHV-2aFLS WT, rec, A, etc.) as described in the legend to Fig. 2A, except the cells had been pretreated with heparinase I for 1.5 h before the inoculation (A) or the recombinant viruses had been incubated with different concentrations of heparin for 1 h at 4°C (B). At 5 h postinfection, the FL activity in the cultures was determined. For each individual recombinant virus, the luciferase expression level observed after mock treatment was set at 100%. Standard deviations (error bars) are indicated.

indicate that viruses carrying the mutations found in the amino terminus of the MHV/BHK S1 subunit, which contribute among others a heparan sulfate-binding consensus sequence, are dependent on heparan sulfate for cell entry.

DISCUSSION

As is the experience with many viruses, establishment and continued passage of cell cultures persistently infected with coronaviruses lead to the accumulation of adaptive mutations, particularly in the spike protein. These mutations can have dramatic effects on the tropism of the virus as was documented clearly by the extended-host-range phenotypes observed with MHV obtained from such cultures (2, 3, 32, 34). While in one case the viruses still used murine CEACAM as a receptor but were dependent on human CEACAM for entry into human cells (2), the MHV variant MHV/BHK generated by Sawicki and Schickli and their coworkers (32, 34) was able to infect cells in a mCEACAM1a-independent (34) and heparan sulfate-dependent manner (11). In the present study we have analyzed in more detail to which regions in the S protein the mutations map that are responsible for the extended-host-range phenotype of MHV/BHK. As it appears, this feature is mainly determined by mutations in two widely separated regions of the S protein, namely, the amino-terminal (A) and FP/HR1 (C) regions. The phenotype was, however, expressed only when the mutations from both these two regions were

jointly present, as virus carrying the mutations of either region alone hardly exhibited the extended host range. Therefore, the two regions seem to communicate and may even interact physically in higher-order structures.

The native conformation of the coronavirus virion S protein is metastable. Binding of the S protein to its receptor triggers conformational changes that facilitate virus entry (19, 25, 28, 49). The stability of the MHV spike can be probed in vitro by incubation of the virus at 37°C under alkaline conditions (43, 49), circumstances that markedly reduce viral infectivity (36). Our observations show that concomitant with the acquisition of the extended host range of MHV/BHK, the accumulated mutations had additionally increased the stability of the spike, a characteristic likely to be selected for during passaging of persistently infected cells. Both the mutations in the S1 subunit (region A) and those in the S2 subunit (region C) were found to contribute to the increased temperature stability. Similar results have been obtained for MHV strain JHM, spikes of which appear to be significantly more unstable at alkaline pH than those of MHV-A59 (42). During passaging in vitro, MHV-JHM variants were selected with an increased S1-S2 stability. Interestingly, the mutations responsible for this phenotype were mapped to two regions of the S protein (19, 22), which correspond to the A and C regions identified in this study.

On the basis of our identification of the three heparan sulfate-binding sites in the MHV/BHK S polypeptide, we hypothesized previously that multiple receptor interactions of the spike protein are probably required to trigger the conformational changes necessary to enable entry of MHV/BHK into HeLa cells (11). We now show that the mutations in S1, of which the extreme amino-terminal part contains the mCEACAM1a-binding domain (23, 38), confer to the recombinant viruses their heparan sulfate dependence, irrespective of their mCEACAM1a dependence. Whether the furin cleavage site in the S protein is functional did not appear to significantly affect entry of HeLa cells (compare MHV-2aFLS A and AB). This unexpected observation is most likely explained by the S proteins in virions carrying cleavable spikes being actually cleaved only poorly, hence leaving a sufficient fraction of the S proteins exposing the heparan sulfate-binding site (11). The putative heparan sulfate-binding site located immediately upstream of the FP clearly enhanced MHV entry into nonmurine cells (compare MHV-2aFLS AC and Ac). In addition, this heparan sulfate-binding motif, which contains several basic amino acids, might also be the target of a cellular protease during entry. Recently, entry of the SARS coronavirus has been demonstrated to be critically dependent on the cellular protease cathepsin L (21, 35), but the actual cleavage site has not yet been determined. Cleavage immediately upstream of the FP would locate this hydrophobic peptide close to the newly generated N terminus of the membrane-anchored subunit, as is the case for all other class I fusion proteins.

Several recombinant viruses generated in this study appear to require two receptor determinants for cell entry. Viruses containing the mutations in the amino-terminal half of the S1 subunit (region A) but lacking those in the FP/HR1 region (region C) are dependent on both heparan sulfate and mCEACAM1a for efficient entry. Entry of these viruses into CEACAM1a-expressing cells was inhibited by antibodies recognizing this receptor: infections carried out at a low MOI could be efficiently blocked (this study), while infections performed at a high MOI were severely delayed (39). Infection could also be inhibited through treatment of cells or viruses with a heparinase or with heparin, respectively. The domain responsible for mCEACAM1a binding is located in the amino-terminal part of the MHV S1 subunit (23, 38); it determines the CEACAM1a receptor specificity of different coronaviruses (42), and amino acid substitutions in this domain can affect mCEACAM1a utilization by MHV-A59 (40). Strikingly, while viruses containing only the mutations in the amino-terminal part of the S1 domain (region A) were able to bind mCEACAM1a approximately to the same extent as viruses that contained only the mutations in the FP/HR1 region (region C), entry of the former but not the latter viruses was negatively affected by removal of cellular heparan sulfate moieties from the cells. Apparently, mCEACAM1a binding alone was not sufficient to induce the required S-protein conformational changes.

Our results indicate that the amino-terminal part of the S protein (region A), including the receptor-binding domain, and a restricted region in the central part of the S protein, containing the HR1 and the putative FP (region C), which are far apart in the linear sequence, are in close contact in the higher-order structures of the spikes. Mutations in these regions appear to have a synergistic effect on S-receptor interaction. Mutations in both regions jointly resulted in reduced binding to mCEACAM1a, increased resistance to inhibition of infection by soluble receptor, increased mCEACAM1a-independent entry, and extended host range. Several other studies have also indicated communication between similar regions in the S1 and S2 subunits. For example, MHV variants resistant against inhibition by soluble receptor had single-amino-acid mutations in either the receptor-binding domain or HR1 domain or immediately downstream thereof (31). Furthermore, the lack of hepatotropism caused by a single mutation in the receptor-binding domain of the MHV-A59 S protein could be overcome by a single-residue substitution in HR1 (29). In addition, it was shown that a combination of mutations, one in the receptor-binding domain and one in HR1, was important for efficient entry of MHV-JHM into mCEACAM1b-expressing cells (27). The obligatory coevolvement of different regions of the S protein was also demonstrated by Tsai and coworkers (42), who constructed viruses with chimeric spikes composed of MHV-4 and MHV-A59 S proteins. While viruses that contain MHV-4 spikes are able to induce receptor-independent fusion, this was not the case for viruses carrying chimeric spikes of MHV-4 and MHV-A59, in which only the receptor-binding domain had been exchanged (42).

Clearly, further interpretation of the data has to await structure information on the coronavirus S protein, especially of its native prefusion form. This information is presently lacking. The only structural data available so far is of the HR1/HR2 complex (17, 37, 45, 46), which forms a heterotrimeric six-helix bundle. Recently, a central cavity has been identified in a crystal structure of the HR1/HR2 complex of SARS coronavirus (17). This cavity is thought to have a destabilizing effect on the complex, which is compensated from the outside by the presence of HR2. The residues lining the cavity in the postfusion form were suggested to be important for an alternative

conformation of the protein, which occurs before the conformational change that leads to fusion (17). Strikingly, the mutations found in the HR1 domain of MHV/BHK appear to cluster around this central cavity. We speculate that in the native fusion protein, the amino-terminal part of the HR1 region is not part of the coiled coil but has an extended secondary structure that folds back towards the S1 subunit, allowing the fusion peptide to reside in the S1 globular head, analogous to the situation in the prefusion state of the paramyxovirus fusion protein (48). In such a conformation, it is conceivable that mutations in the HR1 domain can affect the ability of the S1 subunit to bind to its receptor.

ACKNOWLEDGMENTS

We acknowledge Kay Holmes, Stan Sawicki, and Tom Gallagher for kindly providing MHV-rec1, plasmid constructs, and anti-mCEACAM1a antibodies. We thank Bert Jan Haijema and Fleur de Haan for stimulating discussions.

This work was supported by grants from The Netherlands Organization for Scientific Research (NWO-VIDI-700.54.421) and the China Scholarship Council to C.A.M.D.H. and Z.L., respectively.

REFERENCES

1. **Babcock, G. J., D. J. Esshaki, W. D. Thomas, and D. M. Ambrosino.** 2004. Amino acids 270 to 510 of the severe acute respiratory syndrome coronavirus spike protein are required for interaction with receptor. J. Virol. **78:**4552–4560.
2. **Baric, R. S., E. Sullivan, L. Hensley, B. Yount, and W. Chen.** 1999. Persistent infection promotes cross-species transmissibility of mouse hepatitis virus. J. Virol. **73:**638–649.
3. **Baric, R. S., B. Yount, L. Hensley, S. A. Peel, and W. Chen.** 1997. Episodic evolution mediates interspecies transfer of a murine coronavirus. J. Virol. **71:**1946–1955.
4. **Bonavia, A., B. D. Zelus, D. E. Wentworth, P. J. Talbot, and K. V. Holmes.** 2003. Identification of a receptor-binding domain of the spike glycoprotein of human coronavirus HCoV-229E. J. Virol. **77:**2530–2538.
5. **Bosch, B. J., B. E. Martina, R. Van Der Zee, J. Lepault, B. J. Haijema, C. Versluis, A. J. Heck, R. De Groot, A. D. Osterhaus, and P. J. Rottier.** 2004. Severe acute respiratory syndrome coronavirus (SARS-CoV) infection inhibition using spike protein heptad repeat-derived peptides. Proc. Natl. Acad. Sci. USA **101:**8455–8460.
6. **Bosch, B. J., R. van der Zee, C. A. de Haan, and P. J. Rottier.** 2003. The coronavirus spike protein is a class I virus fusion protein: structural and functional characterization of the fusion core complex. J. Virol. **77:**8801–8811.
7. **Breslin, J. J., I. Mork, M. K. Smith, L. K. Vogel, E. M. Hemmila, A. Bonavia, P. J. Talbot, H. Sjostrom, O. Noren, and K. V. Holmes.** 2003. Human coronavirus 229E: receptor binding domain and neutralization by soluble receptor at 37°C. J. Virol. **77:**4435–4438.
8. **Cavanagh, D.** 1995. The coronavirus surface glycoprotein, p. 73–113. *In* S. G. Siddell (ed.), The coronaviridae. Plenum Press, New York, N.Y.
9. **de Groot, R. J., J. Maduro, J. A. Lenstra, M. C. Horzinek, B. A. van der Zeijst, and W. J. Spaan.** 1987. cDNA cloning and sequence analysis of the gene encoding the peplomer protein of feline infectious peritonitis virus. J. Gen. Virol. **68:**2639–2646.
10. **de Haan, C. A., B. J. Haijema, D. Boss, F. W. Heuts, and P. J. Rottier.** 2005. Coronaviruses as vectors: stability of foreign gene expression. J. Virol. **79:**12742–12751.
11. **de Haan, C. A., Z. Li, E. te Lintelo, B. J. Bosch, B. J. Haijema, and P. J. M. Rottier.** 2005. Murine coronavirus with an extended host range uses heparan sulfate as an entry receptor. J. Virol. **79:**14451–14456.
12. **de Haan, C. A., P. S. Masters, X. Shen, S. Weiss, and P. J. Rottier.** 2002. The group-specific murine coronavirus genes are not essential, but their deletion, by reverse genetics, is attenuating in the natural host. Virology **296:**177–189.
13. **de Haan, C. A., L. van Genne, J. N. Stoop, H. Volders, and P. J. Rottier.** 2003. Coronaviruses as vectors: position dependence of foreign gene expression. J. Virol. **77:**11312–11323.
14. **de Haan, C. A., H. Vennema, and P. J. Rottier.** 2000. Assembly of the coronavirus envelope: homotypic interactions between the M proteins. J. Virol. **74:**4967–4978.
15. **de Haan, C. A. M., and P. J. M. Rottier.** 2005. Molecular interactions in the assembly of coronaviruses, p. 165–230. *In* P. Roy (ed.), Virus structure and assembly, vol. 64. Elsevier Academic Press, San Diego, Calif.
16. **de Haan, C. A. M., K. Stadler, G.-J. Godeke, B. J. Bosch, and P. J. M. Rottier.** 2004. Cleavage inhibition of the murine coronavirus spike protein by a furin-like enzyme affects cell-cell but not virus-cell fusion. J. Virol. **78:**6048–7854.
17. **Duquerroy, S., A. Vigouroux, P. J. Rottier, F. A. Rey, and B. J. Bosch.** 2005. Central ions and lateral asparagine/glutamine zippers stabilize the post-fusion hairpin conformation of the SARS coronavirus spike glycoprotein. Virology **335:**276–285.
18. **Dveksler, G. S., M. N. Pensiero, C. B. Cardellichio, R. K. Williams, G. S. Jiang, K. V. Holmes, and C. W. Dieffenbach.** 1991. Cloning of the mouse hepatitis virus (MHV) receptor: expression in human and hamster cell lines confers susceptibility to MHV. J. Virol. **65:**6881–6891.
19. **Gallagher, T. M.** 1997. A role for naturally occurring variation of the murine coronavirus spike protein in stabilizing association with the cellular receptor. J. Virol. **71:**3129–3137.
20. **Godet, M., J. Grosclaude, B. Delmas, and H. Laude.** 1994. Major receptor-binding and neutralization determinants are located within the same domain of the transmissible gastroenteritis virus (coronavirus) spike protein. J. Virol. **68:**8008–8016.
21. **Huang, I. C., B. J. Bosch, F. Li, W. Li, K. H. Lee, S. Ghiran, N. Vasilieva, T. S. Dermody, S. C. Harrison, P. R. Dormitzer, M. Farzan, P. J. Rottier, and H. Choe.** 2006. SARS coronavirus, but not human coronavirus NL63, utilizes cathepsin L to infect ACE2-expressing cells. J. Biol. Chem. **281:**3198–3203.
22. **Krueger, D. K., S. M. Kelly, D. N. Lewicki, R. Ruffolo, and T. M. Gallagher.** 2001. Variations in disparate regions of the murine coronavirus spike protein impact the initiation of membrane fusion. J. Virol. **75:**2792–2802.
23. **Kubo, H., Y. K. Yamada, and F. Taguchi.** 1994. Localization of neutralizing epitopes and the receptor-binding site within the amino-terminal 330 amino acids of the murine coronavirus spike protein. J. Virol. **68:**5403–5410.
24. **Kuo, L., G. J. Godeke, M. J. Raamsman, P. S. Masters, and P. J. Rottier.** 2000. Retargeting of coronavirus by substitution of the spike glycoprotein ectodomain: crossing the host cell species barrier. J. Virol. **74:**1393–1406.
25. **Lewicki, D. N., and T. M. Gallagher.** 2002. Quaternary structure of coronavirus spikes in complex with carcinoembryonic antigen-related cell adhesion molecule cellular receptors. J. Biol. Chem. **277:**19727–19734.
26. **Liu, J., and S. C. Thorp.** 2002. Cell surface heparan sulfate and its roles in assisting viral infections. Med. Res. Rev. **22:**1–25.
27. **Matsuyama, S., and F. Taguchi.** 2002. Communication between S1N330 and a region in S2 of murine coronavirus spike protein is important for virus entry into cells expressing CEACAM1b receptor. Virology **295:**160–171.
28. **Matsuyama, S., and F. Taguchi.** 2002. Receptor-induced conformational changes of murine coronavirus spike protein. J. Virol. **76:**11819–11826.
29. **Navas-Martin, S., S. T. Hingley, and S. R. Weiss.** 2005. Murine coronavirus evolution in vivo: functional compensation of a detrimental amino acid substitution in the receptor binding domain of the spike glycoprotein. J. Virol. **79:**7629–7640.
30. **Rottier, P., J. Armstrong, and D. I. Meyer.** 1985. Signal recognition particle-dependent insertion of coronavirus E1, an intracellular membrane glycoprotein. J. Biol. Chem. **260:**4648–4652.
31. **Saeki, K., N. Ohtsuka, and F. Taguchi.** 1997. Identification of spike protein residues of murine coronavirus responsible for receptor-binding activity by use of soluble receptor-resistant mutants. J. Virol. **71:**9024–9031.
32. **Sawicki, S. G., J. H. Lu, and K. V. Holmes.** 1995. Persistent infection of cultured cells with mouse hepatitis virus (MHV) results from the epigenetic expression of the MHV receptor. J. Virol. **69:**5535–5543.
33. **Schickli, J. H., L. B. Thackray, S. G. Sawicki, and K. V. Holmes.** 2004. The N-terminal region of the murine coronavirus spike glycoprotein is associated with the extended host range of viruses from persistently infected murine cells. J. Virol. **78:**9073–9083.
34. **Schickli, J. H., B. D. Zelus, D. E. Wentworth, S. G. Sawicki, and K. V. Holmes.** 1997. The murine coronavirus mouse hepatitis virus strain A59 from persistently infected murine cells exhibits an extended host range. J. Virol. **71:**9499–9507.
35. **Simmons, G., D. N. Gosalia, A. J. Rennekamp, J. D. Reeves, S. L. Diamond, and P. Bates.** 2005. Inhibitors of cathepsin L prevent severe acute respiratory syndrome coronavirus entry. Proc. Natl. Acad. Sci. USA **102:**11876–11881.
36. **Sturman, L. S., C. S. Ricard, and K. V. Holmes.** 1990. Conformational change of the coronavirus peplomer glycoprotein at pH 8.0 and 37°C correlates with virus aggregation and virus-induced cell fusion. J. Virol. **64:**3042–3050.
37. **Supekar, V. M., C. Bruckmann, P. Ingallinella, E. Bianchi, A. Pessi, and A. Carfi.** 2004. Structure of a proteolytically resistant core from the severe acute respiratory syndrome coronavirus S2 fusion protein. Proc. Natl. Acad. Sci. USA **101:**17958–17963.
38. **Suzuki, H., and F. Taguchi.** 1996. Analysis of the receptor-binding site of murine coronavirus spike protein. J. Virol. **70:**2632–2636.
39. **Thackray, L. B., and K. V. Holmes.** 2004. Amino acid substitutions and an insertion in the spike glycoprotein extend the host range of the murine coronavirus MHV-A59. Virology **324:**510–524.
40. **Thackray, L. B., B. C. Turner, and K. V. Holmes.** 2005. Substitutions of conserved amino acids in the receptor-binding domain of the spike glycoprotein affect utilization of murine CEACAM1a by the murine coronavirus MHV-A59. Virology **334:**98–110.
41. **Thorp, E. B., and T. M. Gallagher.** 2004. Requirements for CEACAMs and cholesterol during murine coronavirus cell entry. J. Virol. **78:**2682–2692.
42. **Tsai, J. C., B. D. Zelus, K. V. Holmes, and S. R. Weiss.** 2003. The N-terminal

domain of the murine coronavirus spike glycoprotein determines the CEACAM1 receptor specificity of the virus strain. J. Virol. **77:**841–850.
43. **Weismiller, D. G., L. S. Sturman, M. J. Buchmeier, J. O. Fleming, and K. V. Holmes.** 1990. Monoclonal antibodies to the peplomer glycoprotein of coronavirus mouse hepatitis virus identify two subunits and detect a conformational change in the subunit released under mild alkaline conditions. J. Virol. **64:**3051–3055.
44. **Wong, S. K., W. Li, M. J. Moore, H. Choe, and M. Farzan.** 2004. A 193-amino acid fragment of the SARS coronavirus S protein efficiently binds angiotensin-converting enzyme 2. J. Biol. Chem. **279:**3197–3201.
45. **Xu, Y., Y. Liu, Z. Lou, L. Qin, X. Li, Z. Bai, H. Pang, P. Tien, G. F. Gao, and Z. Rao.** 2004. Structural basis for coronavirus-mediated membrane fusion. Crystal structure of mouse hepatitis virus spike protein fusion core. J. Biol. Chem. **279:**30514–30522.
46. **Xu, Y., Z. Lou, Y. Liu, H. Pang, P. Tien, G. F. Gao, and Z. Rao.** 2004. Crystal structure of severe acute respiratory syndrome coronavirus spike protein fusion core. J. Biol. Chem. **279:**49414–49419.
47. **Ye, R., C. Montalto-Morrison, and P. S. Masters.** 2004. Genetic analysis of determinants for spike glycoprotein assembly into murine coronavirus virions: distinct roles for charge-rich and cysteine-rich regions of the endodomain. J. Virol. **78:**9904–9917.
48. **Yin, H. S., X. Wen, R. G. Paterson, R. A. Lamb, and T. S. Jardetzky.** 2006. Structure of the parainfluenza virus 5 F protein in its metastable, prefusion conformation. Nature **439:**38–44.
49. **Zelus, B. D., J. H. Schickli, D. M. Blau, S. R. Weiss, and K. V. Holmes.** 2003. Conformational changes in the spike glycoprotein of murine coronavirus are induced at 37°C either by soluble murine CEACAM1 receptors or by pH 8. J. Virol. **77:**830–840.